Communication

Observing Single Nanoparticle Collisions at an Ultramicroelectrode by Electrocatalytic Amplification

Xiaoyin Xiao, and Allen J. Bard

J. Am. Chem. Soc., **2007**, 129 (31), 9610-9612• DOI: 10.1021/ja072344w • Publication Date (Web): 14 July 2007

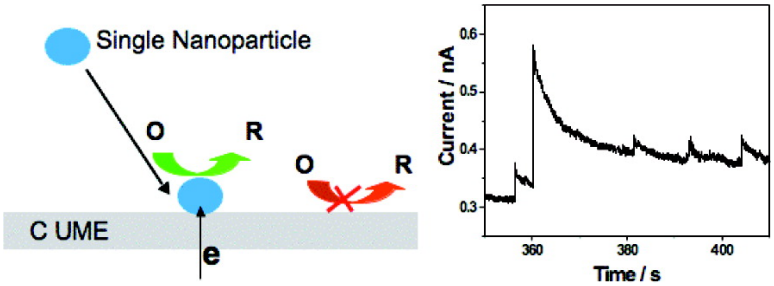

More About This Article

Additional resources and features associated with this article are available within the HTML version:

- Supporting Information
- Links to the 5 articles that cite this article, as of the time of this article download
- Access to high resolution figures
- Links to articles and content related to this article
- Copyright permission to reproduce figures and/or text from this article

View the Full Text HTML

J|A|C|S COMMUNICATIONS

Published on Web 07/14/2007

Observing Single Nanoparticle Collisions at an Ultramicroelectrode by Electrocatalytic Amplification

Xiaoyin Xiao and Allen J. Bard*

Center for Electrochemistry, Center for Nano and Molecular Science, Department of Chemistry and Biochemistry, University of Texas at Austin, 1 University Station A5300, Austin, Texas 78712-0165

Received April 3, 2007; E-mail: ajbard@mail.utexas.edu

We describe a simple method for observing electrochemically the collisions of single metal nanoparticles (NPs) at an electrode. This can provide a useful approach to the study of electrocatalysis at single metal NPs, as well as the basis of highly sensitive electroanalytical methods. Metal NPs have a wide range of applications in electronics, optics, and catalysis. While most of this research has focused on the properties of particle ensembles,[1−4] the exploration at the single particle level has also been of interest.[5−8] Experimental difficulties at the single particle level usually involve problems in generating, locating, and characterizing a single NP, especially at the nm scale and in measuring the very small currents or charges associated with these electrode reactions.[9]

The method proposed here is based on the large current amplification factor involved in a rapid electrocatalytic reaction of a species in single particle collision events. The reaction at the NP of the species at a relatively high concentration in solution does not occur at the conductive measuring ultramicroelectrode (UME) [which is not catalytic] (Figure 1a). As an example, consider a carbon fiber UME immersed in a dispersion of Pt NPs in an acidic aqueous solution. The steady-state diffusion-controlled flux of particles to the UME surface, $J_{p,s}$, when the particles adhere to the surface, is given by

$$J_{p,s} = 4D_pC_p/\pi a \quad (1)$$

where D_p is the particle diffusion coefficient, C_p is the particle concentration, and a is the radius of the carbon UME disk electrode.[10] Ordinarily, in the simple NP charging process, only one or a few electrons would transfer between the NP and the UME (n_p) to yield a current, $i_{p,s} = n_pF\pi a^2J_{p,s}$, that is much too small to observe above the noise and background level (where F is the Faraday). However if the NP can electrocatalyze another reaction, say reduction of a species O to R, upon contact with the UME (e.g., hydrogen evolution at a Pt particle), a much larger current, i_O, can flow. That is, when the NP collides and sticks to the electrode surface, it allows the reaction of O to R at a potential where this reaction does not occur at the UME. For example, the steady-state diffusion-controlled current at a particle on the surface is given by

$$i_O = n_OFA_p\,J_{O,p} = Bn_OFD_OC_Or_0 \quad (2)$$

where $J_{O,p}$ is the flux of O to the particle, D_O is the diffusion coefficient of O in the solution, C_O is the concentration of O, and r_0 is the radius of the particle. The factors, A_p, the particle area, and B, depend on the particle shape and how it is situated on the UME. If it can be considered a sphere on an infinite plane, then $A_p = 4\pi r_0^2$ and $B = 4\pi \ln 2 = 8.71$.[11] Since C_O and D_O can be much larger than C_p and D_p, even with the difference in a and r_0, the diffusional flux of O to a single particle can be 10 orders of magnitude or more larger than that of particles to the UME.

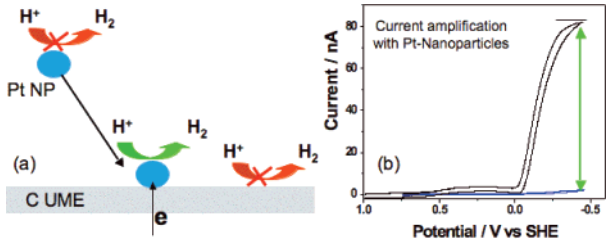

Figure 1. (a) Schematic of a single platinum nanoparticle collision event: a particle diffuses to the electrode, collides, and catalyzes proton reduction during the residence time. (b) Electrochemical reduction of proton at carbon fiber electrode without (blue) and with (black) Pt nanoparticles on the surface in air-saturated, 50 mM sodium dihydrogencitrate solution (fiber diameter, 8 μm; sweep rate, 100 mV/s).

In actuality, the current for a collision is a transient that includes particle charging and a changing faradaic current for O reduction that attains steady state in a time of $\sim r_0^2/D_O$. Since different types of collisions can occur, the current−time ($i-t$) transient for each collision event will be determined by the residence time, τ, of the particle at the electrode, that is, the time period when the electrode can pass electrons to the particle. If the particle sticks to the electrode for a time sufficient for a steady-state current to be attained, and the reactant O is only reduced at the particle, an amplification factor given by the relative steady-state fluxes of the particles and O, is $\sim(B/16)(D_OC_Oa)/(D_pC_p\ r_0)$. This will lead to relative steady-state currents of $\sim B(D_OC_Or_0)/4(D_pC_pa)$ (assuming $n_p = n_O$). For a 1 pM particle solution and 10 mM indicator O, the estimated amplification factor for a 1 nm radius particle can be nine to 10 orders of magnitude, assuming the diffusion coefficient of reactant O and that of the particle are different by about an order of magnitude.

Two electrochemical reactions, the reduction of proton and the reduction of hydrogen peroxide, were chosen to illustrate this effect. Both of these reactions are sluggish at a carbon UME but are more rapid at Pt. As shown in Figure 1b, proton reduction does not occur at a carbon electrode in 50 mM sodium dihydrogen citrate (NaH_2-Citr) at potentials positive of −0.5 V versus SHE (standard hydrogen electrode); the small increase in current between 0 and −0.5 V is due to some reduction of oxygen in the solution. For a carbon electrode covered with Pt particles or a pure Pt electrode, proton reduction gives rise to a steady-state current at potentials more negative than −0.3 V.[12] At these potentials, oxygen reduction is also significantly promoted. The steady-state current at a Pt particle can be estimated from the steady-state current to a sphere in contact with a nonreacting plane, provided the particle maintains ohmic contact with the UME and the applied potential is sufficient to change O to R under diffusion control. This current for proton reduction under the described conditions should be about 30 pA for a spherical particle of 2 nm in diameter. Higher currents per particle could be achieved by increasing the proton concentration,

10.1021/ja072344w CCC: $37.00

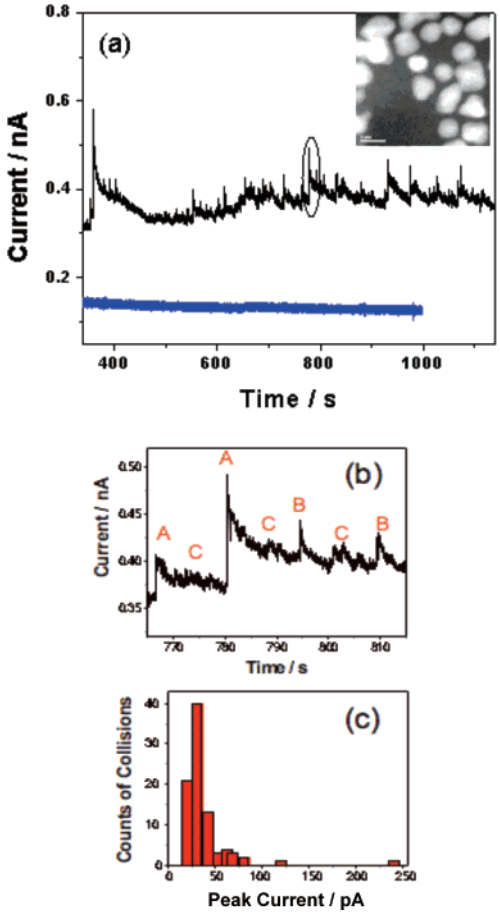

Figure 2. (a) Current transients at a carbon fiber electrode in 50 mM sodium dihydrogencitrate solution in the absence (blue) and presence (black) of Pt citrate nanoparticles. Particle concentration is about 25 pM. (b) Zoom in of panel a showing three kinds of collisions distinguished by the current amplitude and frequency: A, B, C. (c) Statistics of number of collisions versus their peak currents. Collisions with peak currents less than 15 pA, which were typically C type, are not included in this figure, and collisions with peak current larger than 40 pA are mostly due to sticking of the particles. Inset is a TEM image of representative Pt nanoparticles.

for example, using higher concentrations of sodium dihydrogencitrate or using perchloric acid (which must be less than 60 mM to avoid the formation of hydrogen bubbles). However, the particles aggregate and precipitate under these higher acid conditions because of neutralization of the stabilizing negative surface charge (Figure S2).

Figure 2 shows the current transients at a carbon disk UME in a solution before and after injecting Pt particles. Details of the experiments are given in the Supporting Information. Briefly the electrode, made by sealing an 8 μm diameter C fiber in soft glass and then polishing the bottom so that only a disk of C is exposed to the solution, was held at -0.4 V. The Pt colloidal solution was obtained by reducing 2 mM H_2PtCl_6 with sodium borohydride in the presence of sodium citrate.[13] The particle sizes ranged between 2 and 6 nm distributed mainly at 4 ± 0.8 nm in diameter. Assuming a particle contains about 2000 Pt atoms,[14] the stock solution was about 1 μM in particles. Before each experiment the as-prepared Pt colloidal stock solution was diluted a few to 100 times with water. A few μL of this solution was injected into about 50 mL test electrolyte in the electrochemical cell under nitrogen bubbling yielding a particle concentration in the test solution in the pM range. The electrolyte was stirred by nitrogen bubbling for about 10 s after injection with the electrode held above the electrolyte at the desired potential. The $i-t$ response was recorded upon immersion of the C UME into the solution maintained under a nitrogen atmosphere. Before injection of the particle solution, the current transient was a smooth curve at a small constant noise level, while after injection peaked current transients appeared. These current transients are a result of the collisions of particles with the C UME. Additional evidence in support of this explanation is (1) no peaked current transients were observed when noncatalytic carbon nanoparticles were injected (Figure S1, Supporting Information); (2) the amplitude of the steady-state current for an irreversible collision, that is, where a particle sticks to the surface is about 40 to 80 pA, which is about the calculated value for the sizes of particles injected; (3) as shown in Figure S2, the amplitude of the current spikes decreases with a positive shift of the electrode potential, as expected from the steady-state current recorded at the Pt UME (Figure 1b); (4) the proton concentration influences the amplitude of the current spikes; (5) the frequency of the collision was nearly proportional to the particle concentration (Figure S4). The average frequency is about 0.04 per second per pM particle concentration at the C UME used, which is very close to that estimated by eq 1 of 0.03 s^{-1} pM^{-1} particle concentration for an 8 μm carbon electrode, assuming a diffusion coefficient of the particle of 1×10^{-8} cm^2/s; (6) the current amplitude varies with the size of particles injected, larger particles produce bigger spikes, as shown in Figures S5 and S6 for particles bigger than 8 nm and less than 2 nm, respectively.

Particle collisions with the electrode typically give rise to different types of $i-t$ responses, as shown in Figure 2b. Each $i-t$ profile is associated with individual single particle collisions. The characteristics of an individual $i-t$ profile are affected by the particle size, the particle residence time, and the interaction between particle and the electrode surface. The expected $i-t$ profile is a transient with a rapid (<ms) decay to a steady-state level. This is seen at very short times, but for the hydrogen evolution reaction, the current decays over a period of tens of s. This may be caused by deactivation of the particle surface, for example, by adsorption of blocking impurities or because of hydrogen incorporation in the NP. We have seen similar irreversible deactivation of nm size Pt UMEs. As shown below, the $i-t$ curves for H_2O_2 reduction are somewhat closer to the expected behavior. There is also a repulsive interaction between the negatively charged particle and the negatively charged surface. We have examined this effect by setting the potential at even more negative values, where we observed fewer collisions. The different $i-t$ responses are possibly due to the nature of the collisions (e.g., how closely a particle can approach to the electrode surface within a distance where electron tunneling is possible), to the residence time, and also to particle size and shape effects. This needs to be further clarified with additional experiments.

When increasing the proton concentration to 10 mM $HClO_4$, the Pt nanoparticles are not stable, because of protonation of the carboxylic groups of the negative stabilizing citrate. Figure 3 shows some typical current-time transients for individual single particle collisions. Recording current transients under these conditions shows, right after injection of particles, very abrupt spikes that appear during a time interval of less than 600 s (Figure S3), after which the transients disappear because the nm particles aggregate and precipitate.

As a control experiment we also recorded the current transients in the presence of larger Pt nanoparticles, stabilized by oxalate (typically >8 nm diameter) (Figure S6). In these experiments we observed only a few current spikes within the same time period at the same Pt concentration, as expected when both the particle concentration and the particle diffusion coefficient become smaller.

We have also examined single NP collision events using hydrogen peroxide as the indicator instead of proton. To reduce

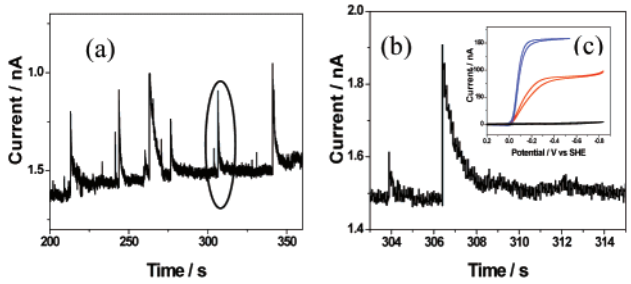

Figure 3. (a) Current transient at a C UME in 10 mM perchloric acid and 20 mM sodium perchlorate in the presence of Pt citrate nanoparticles. Particle concentration is about 12.5 pM. (b) Zoom in of panel a. (c) Cyclic voltammograms of C UME (black) and Pt UME in 50 mM sodium dihydrogencitrate (red) and in 10 mM perchloric acid and 20 mM sodium perchlorate, respectively.

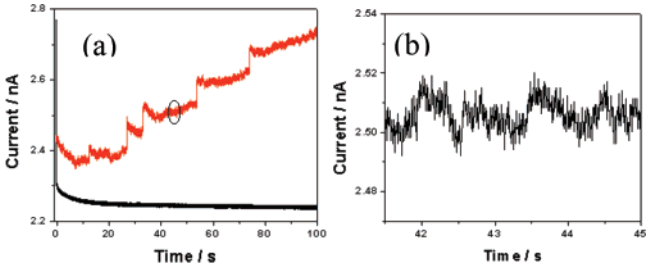

Figure 4. (a) Current transients at a benzenedimethanethiol modified 25 μm diameter gold electrode at 0.1 V versus SHE in 0.1 M PBS pH 7.4 buffer solution containing 50 mM hydrogen peroxide in the absence (black) and presence of 25 pM Pt−NP (red). The background current in black curve was increased by 1.5 nA for clarity. Panel b is a zoom in of panel a.

the background current and promote binding of the particle to the electrode surface, we coated an Au UME (which is not catalytic for H_2O_2 reduction) with a surface assembled monolayer of benzenedimethanethiol, which forms a stable monolayer capable of electron tunneling to solution species.[15] The terminal thiol group can strongly bind to the Pt particles. An instant increase of current is observed upon particle injection due to the proximity of immobilized Pt particles. In addition to the discrete steps in the $i-t$ response, characteristic of sticky collisions, we also observed smaller current fluctuation with smaller amplitudes but with higher frequency. The frequency of these is about 2 orders of magnitude higher than that of the discrete current steps. The fluctuation shown in Figure 4b is analogous to similar collisions observed in proton reduction as shown in Figure 2b (type C) and may be caused by smaller Pt particles in the preparation.

In conclusion, we have demonstrated a novel method of observing single particle collision events with a UME. A single event is characterized by the current generated through the particle-catalyzed reaction of an indicator present in solution. Since the indicator can be selected to have a high concentration and a high diffusion coefficient, large amplification occurs. Every collision produces a unique $i-t$ profile that is a function of the particle interaction with the electrode surface. By modifying the particle concentration, particle size (e.g., Pt citrate nanoparticles vs Pt dendrimer nanoparticles), applied substrate potential, and the concentration of the indicator, it should be possible to use the $i-t$ profiles to obtain information about the indicator reaction at a single particle. In comparison to amplifying optical, conductivity, and mass signals using nanoparticles,[16,17] the catalytic current amplification should allow a study of the dynamics of the process and information about the heterogeneous electron-transfer kinetics at the single-particle level. Thus, in addition to the usual advantage of single-particle studies compared to ensembles of obtaining information about particle environments, this approach may also provide dynamic information not seen in ensembles. Moreover, it might be useful in determining particle size distributions and as a very sensitive electroanalytical method, perhaps to the single-binding event level. Finally, it allows one to carry out electrochemical experiments at very low concentrations where the behavior is statistical and random rather than the conventional (Fickian) response.

Acknowledgment. We appreciate valuable discussions with Drs. R. M. Crooks, F-R. F. Fan, M. Alpuche, J. P. Zhou, and C. Zoski. We also thank Dr. Heechang Ye for his generous supply of Pt dendrimer nanoparticles and the National Science Foundation (Grant CHE 0451494) for their support.

Supporting Information Available: Additional experimental data on changing the applied potential, proton concentration, particle concentration, and different sizes of Pt NP synthesized using G6 dendrimer and oxalate as stabilizing agents. This material is available free of charge via the Internet at http://pubs.acs.org.

References

(1) Chen, S. W.; Ingram, R. S.; Hostetler, M. J.; Pietron, J. J.; Murray, R. W.; Schaaff, T. G.; Khoury, J. T.; Alvarez, M. M.; Whetten, R. L. *Science* **1998**, *280*, 2098−2101.
(2) Narayanan, R.; El-Sayed, M. A. *J. Phys. Chem. B* **2005**, *109*, 12663−12676.
(3) Harnisch, J. A.; Pris, A. D.; Porter, M. D. *J. Am. Chem. Soc.* **2001**, *123*, 5829−5830.
(4) Polsky, R.; Gill, R.; Kaganovsky, L.; Willner, I. *Anal. Chem.* **2006**, *78*, 2268−2271.
(5) Fan, F. R. F.; Bard, A. J. *Science* **1997**, *277*, 1791−1793.
(6) Chen, S. L.; Kucernak, A. *J. Phys. Chem. B* **2003**, *107*, 8392−8402.
(7) Krapf, D.; Wu, M. Y.; Smeets, R. M. M.; Zandbergen, H. W.; Dekker, C.; Lemay, S. G. *Nano Lett.* **2006**, *6*, 105−109.
(8) Tel-Vered, R.; Bard, A. J. *J. Phys. Chem. B* **2006**, *110*, 25279−25287.
(9) Lee, S.; Zhang, Y. H.; White, H. S.; Harrell, C. C.; Martin, C. R. *Anal. Chem.* **2004**, *76*, 6108−6115. Ito, T.; Sun, L.; Crooks, R. M. *Anal. Chem.* **2003**, *75*, 2399−2406.
(10) Bard, A. J.; Faulkner, L. R. *Electrochemcial Methods, Fundamentals and Applications*, 2nd ed.; John Wiley & Sons: New York, 2001.
(11) Bobbert, P. A.; Wind, M. M.; Vlieger, J. *Physica* **1987**, *141A*, 58−72.
(12) Zhou, J. F.; Zu, Y. B.; Bard, A. J. *J. Electroanal. Chem.* **2000**, *491*, 22−29.
(13) Yang, J.; Lee, J. Y.; Too, H. P. *Anal. Chim. Acta* **2006**, *571*, 206−210.
(14) Jentys, A. *Phys. Chem. Chem. Phys.* **1999**, *1*, 4059−4063.
(15) Xiao, X. Y.; Xu, B. Q.; Tao, N. J. *Nano Lett.* **2004**, *4*, 267−271.
(16) Sonnichsen, C.; Reinhard, B. M.; Liphardt, J.; Alivisatos, P. A. *Nat. Biotechnol.* **2005**, *23*, 741−745.
(17) Zhang, Z. L.; Pang, D. W.; Yuan, H.; Cai, R. X.; Abruna, H. *Anal. Bioanal. Chem.* **2005**, *381*, 833−838.

JA072344W